Activity of biogenic silver nanoparticles in planktonic and biofilm-associated *Corynebacterium pseudotuberculosis*

Laerte Marlon Santos[1], Daniela Méria Rodrigues[1], Bianca Vilas Boas Alves[1], Mauricio Alcântara Kalil[1], Vasco Azevedo[2], Debmalya Barh[2,3], Roberto Meyer[1], Nelson Duran[4], Ljubica Tasic[5] and Ricardo Wagner Portela[1]

[1] Instituto de Ciencias da Saude, Universidade Federal da Bahia, Salvador, Bahia, Brazil
[2] Instituto de Ciencias Biologicas, Universidade Federal de Minas Gerais, Belo Horizonte, Minas Gerais, Brazil
[3] Institute of Integrative Omics and Applied Biotechnology, Nonakuri, West Bengal, India
[4] Instituto de Biologia, Universidade Estadual de Campinas, Campinas, Sao Paulo, Brazil
[5] Instituto de Quimica, Universidade Estadual de Campinas, Campinas, Sao Paulo, Brazil

ABSTRACT

Corynebacterium pseudotuberculosis is a gram-positive bacterium and is the etiologic agent of caseous lymphadenitis (CL) in small ruminants. This disease is characterized by the development of encapsulated granulomas in visceral and superficial lymph nodes, and its clinical treatment is refractory to antibiotic therapy. An important virulence factor of the *Corynebacterium* genus is the ability to produce biofilm; however, little is known about the characteristics of the biofilm produced by *C. pseudotuberculosis* and its resistance to antimicrobials. Silver nanoparticles (AgNPs) are considered as promising antimicrobial agents, and are known to have several advantages, such as a broad-spectrum activity, low resistance induction potential, and antibiofilm activity. Therefore, we evaluate herein the activity of AgNPs in *C. pseudotuberculosis*, through the determination of minimum inhibitory concentration (MIC), minimum bactericidal concentration (MBC), antibiofilm activity, and visualization of AgNP-treated and AgNP-untreated biofilm through scanning electron microscopy. The AgNPs were able to completely inhibit bacterial growth and inactivate *C. pseudotuberculosis* at concentrations ranging from 0.08 to 0.312 mg/mL. The AgNPs reduced the formation of biofilm in reference strains and clinical isolates of *C. pseudotuberculosis,* with interference values greater than 80% at a concentration of 4 mg/mL, controlling the change between the planktonic and biofilm-associated forms, and preventing fixation and colonization. Scanning electron microscopy images showed a significant disruptive activity of AgNP on the consolidated biofilms. The results of this study demonstrate the potential of AgNPs as an effective therapeutic agent against CL.

Subjects Microbiology, Veterinary Medicine

Keywords Antimicrobial agent, Caseous lymphadenitis, Nanotechnology, Small ruminants, Complementary treatment

Submitted 11 September 2023
Accepted 13 December 2023
Published 20 February 2024

Corresponding author
Ricardo Wagner Portela,
rwportela@ufba.br

Academic editor
Jonathan Thomas

Additional Information and Declarations can be found on page 14

DOI **10.7717/peerj.16751**

INTRODUCTION

Corynebacterium pseudotuberculosis is a gram-positive pathogen that has great veterinary importance since it is the etiologic agent of caseous lymphadenitis (CL) in small ruminants

How to cite this article Santos LM, Rodrigues DM, Alves BVB, Kalil MA, Azevedo V, Barh D, Meyer R, Duran N, Tasic L, Portela RW. 2024. Activity of biogenic silver nanoparticles in planktonic and biofilm-associated *Corynebacterium pseudotuberculosis*. *PeerJ* **12**:e16751
http://doi.org/10.7717/peerj.16751

(*Dorella et al., 2006*). CL is mainly characterized by the development of encapsulated granulomas in visceral and superficial lymph nodes, as well as in organs such as liver, lungs, spleen, and kidneys (*Barral et al., 2022*). As *C. pseudotuberculosis* is a zoonotic agent, it is important to consider CL as a public health problem, since cases of infection in humans were already described in several countries, such as Australia, New Zealand, and France (*Bastos et al., 2012*).

CL is refractory to antibiotic therapy because of the development of a thick capsule around the lesions, and as a consequence of the cheesy nature of the granuloma's content. Also, antibiotics can only eliminate the pathogen from superficial lesions, and internal lesions and/or abscesses may not be affected by the treatment and remain active, causing recurrences (*Williamson, 2001*; *Fontaine & Baird, 2008*).

The ability of the bacteria from *Corynebacterium* genus to produce biofilm is considered as an important virulence factor (*Guedes et al., 2015*). This structure is an aggregate of microcolonies surrounded by a matrix composed by polysaccharides, forming organized communities that allow adhesion to biological surfaces, and is characterized by an enhanced resistance to antimicrobials (*Vestby et al., 2020*) and biocides (*Sá et al., 2013*) in the chronic stage of the disease.

Currently, there is a need to develop new alternatives for the treatment and control of infectious diseases, and silver nanoparticles (AgNPs) are being considered as promising antimicrobial agents, since it exhibits several advantages, such as broad-spectrum and wound healing activities, and a low potential of resistance induction (*Tăbăran et al., 2020*; *Fernandez et al., 2021*). AgNPs produced using *Fusarium oxysporum* biomass have already proven to have significant antimicrobial activity against *Candida* sp., not only *in vitro* (*Fonseca et al., 2022*) but also *in vivo* (*Fonseca et al., 2023*). A previous study found that biogenic AgNPs were able to accelerate the wound healing process after the surgical excision of caseous lymphadenitis lesions (*Santos et al., 2019*). Therefore, we aimed herein to evaluate the antibiofilm and antibacterial activity of AgNPs in *C. pseudotuberculosis* clinical isolates and reference strains.

MATERIALS & METHODS

Biogenic AgNP synthesis and characterization

The AgNPs were synthetized as described by *Ballottin et al. (2017)*. The *Fusarium oxysporum* fungus was cultivated in a solid culture medium (2% malt, 2% agar, 0.5% yeast extract and distilled water), and was incubated for one week at 28 °C. Then, sterile milliQ water was added to the culture until a 0.1 g/mL protein concentration was reached, and kept under agitation for 72 h. Then, the supernatant was the filtered and 0.01 mol/L of $AgNO_3$ was added. The solution was sealed with aluminum foil and kept at 28 °C until the formation of the nanoparticles.

The morphology of the AgNPs was observed using a Zeiss CEM-902 (Zeis, Oberkochen, Germany) transmission electron microscope set at 80 keV. The zeta potential of the AgNPs was obtained by electrophoretic mobility, through the dispersion of the AgNP in a KCl solution. The surface charge was measured using a Zetasizer Nano series equipment (Malvern Instruments, Malvern, UK) (*Ballottin et al., 2017*)

Bacterial strains

Four *C. pseudotuberculosis* reference strains were used in this study: the 1002 strain, which was used as a reference for the bacterial genome project (*Mariano et al., 2016*); the N1 strain, which is a viscerotropic strain isolated from a lung lesion of a sheep with CL (*Loureiro et al., 2016*); the T1 strain, an attenuated strain used as a vaccine model (*Moura-Costa et al., 2008*); and the CAPJ4 strain, a strain previously described as biofilm-producing (*De Sá et al., 2021*). All these strains belong to the biovar ovis and have already their genome sequenced and deposited (GenBank accession numbers CP001809.2, CP013146, CP015100.1 and CP026499, respectively). Four clinical isolates obtained from caseous samples of sheep subjected to CL lesion excision (*Kalil et al., 2019*) were molecularly identified using quadruplex PCR (*Almeida et al., 2017*), and were also included in this study.

Determination of minimal inhibitory concentration (MIC) and minimal bactericidal concentration (MBC)

The broth microdilution methodology was performed as previously described by *Norman et al. (2014)*, with modifications. The solution containing the AgNPs was diluted in sterile milli-Q (concentrations ranging from 0.01 to 5 mg/mL). The *C. pseudotuberculosis* strains were then inoculated in brain heart infusion broth—BHI (HIMEDIA, Mumbai, India) added with 0.1% Tween 80 and incubated for 24 h. After this step, the strains were diluted in 2 × BHI until an optical density of 0.08–0.10 at 600 nm was achieved (which contains approximately 2×10^6 CFU/mL of the bacteria). These suspensions were then diluted in 2× BHI broth (concentration of 1×10^6 CFU/mL). After dilution, 100 µL of the AgNP colloidal solution in different concentrations and 100 µL of the inoculum were inoculated into a 96-well flat-bottom polystyrene microplate. The culture microplates were consequently incubated at 37 °C for 48 h. As controls, the AgNP-not treated *C. pseudotuberculosis* bacterial suspension was used as a positive control, and the colloidal solution of AgNPs without the addition of bacteria was considered as a negative control. After a final 600 nm read at a spectrophotometer (Bio-Rad, Hercules, CA, USA), it was possible to determine the minimum concentration of AgNP that was able to fully inhibit the bacterial growth (MIC_{100}). In addition, Petri dishes containing BHI agar were inoculated with 20 µL taken from each well of the culture microplates used for the MIC_{100} determination, followed by an incubation for 48 h at 37 °C, and then the minimal concentration of the AgNPs that was able to fully inactivate the bacteria (MBC_{100}) was established. The MIC_{100} and the MBC_{100} assays were repeated three times.

Biofilm production assay

This semiquantitative methodology was conducted as previously described by *Kalil et al. (2019)*. A *C. pseudotuberculosis* bacterial suspension was inoculated in tryptone soy broth (TSB) and incubated at 37 °C. 200 µL of the bacterial suspension were transferred to culture microplates and incubated for 48 h at 37 °C. Then, the wells were aspirated and washed twice with sterile PBS. The material that remained attached to the plate was then fixed with methanol and dried. The biofilms were stained with a 2% crystal violet solution

for 5 min and washed with 0.01 M PBS pH 7.2. The dye was then eluted with a 33% acetic acid solution. As a negative control, it was used the content of wells with the broth and without the inoculum. The 595 nm OD from each well was then measured.

The following equations were used to characterize the intensity of biofilm formation, where ODI indicates the optical density of the isolate, and ODNC represents the optical density of the negative control: ODI $\leq$ ODNC = no biofilm development; ODI/ODNC $\leq$ 2 = weak biofilm formation; ODI/ODNC $\leq$ 4 = moderate biofilm production capacity; ODI/ODNC >4 = strong biofilm production capacity (*Nostro et al., 2007*). The CAPJ4 strain of *C. pseudotuberculosis* was used as a biofilm-forming control strain (*Sá et al., 2018*). Three independent experiments were performed.

Determination of minimal inhibitory concentration for consolidated biofilms (MIBC)

The AgNPs antibiofilm action assay was conducted as previously described by *Santos et al. (2021)*. The *C. pseudotuberculosis* isolates were inoculated in TSB and incubated at 37 °C for 48 h. The bacterial suspensions were then standardized to a 595 nm OD of 0.2, and 200 µL were transferred to culture microplate wells and incubated for 48 h at 37 °C. After the consolidation of the biofilm, and taking into consideration the optimal concentrations previously obtained in the minimal inhibitory concentration (MIC) assays, the bacterial inoculum used for biofilm formation, and the fact that concentrations of up to 16x MIC were previously described as needed to observe antibiofilm action (*De Oliveira et al., 2016*; *Trevisan et al., 2018*; *Shrestha et al., 2022*), 200 uL of the AgNP solutions (0.25, 0.5, 1, 2 and 4 mg/mL) were added to the wells. The microplates were then incubated for 48 h at 37 °C. The 595 nm OD was determined right after the addition of the AgNP (OD 0 h), 24 h (OD 24 h), and 48 h (OD 48 h) after. The MIBC was then characterized as the lowest antimicrobial concentration in which there was no time-dependent increase in the biofilm content when an early exposure time was compared with a later exposure time (*Macià, Rojo-Molinero & Oliver, 2014*). Different controls were included in the experiment: a negative control, composed by biofilm and Milli-Q water; a control with TSB broth and each AgNP dilution; and a control made only with TSB broth. Three independent experiments were performed.

Determination of AgNP interference on biofilm formation

C. pseudotuberculosis isolates were inoculated in TSB and incubated at 37 °C for 48 h. The bacterial suspensions were then standardized to a 595 nm OD of 0.2. 100 µL of the AgNP solutions (0.25, 0.5, 1, 2 and 4 mg/mL) were mixed with 100 µL of these standardized bacterial suspensions and added to culture microplates, and incubated at for 48 h for 37 °C. After 48 h, the biofilm was detected and the percentage of inhibition of biofilm production was calculated considering the control bacterial suspensions that were not incubated with the AgNPs (*Kalil et al., 2019*). Three independent trials were performed.

The percentage of inhibition of the biofilm formation was calculated using a formula previously described (*Siddique et al., 2020*; *Santos et al., 2021*), as follows:

$$\%\ \text{inhibition} = 1 - \frac{\text{OD595 of the treated } C.pseudotuberculosis}{\text{OD595 of the not} - \text{treated } C.pseudotuberculosis} \times 100.$$

Scanning electron microscopy (SEM)

The bacterial biofilms (AgNP-treated and -untreated) were obtained using the methodologies described herein; however, a sterile glass coverslip was added to each well of the culture plate, and the coverslips containing the biofilms were then analyzed at the scanning electron microscope. The biofilms (treated or not with the AgNPs at 4 mg/mL) were fixed in (i) 2.5% glutaraldehyde in 0.1 M sodium cacodylate pH 7.4 for 2 h, and (ii) 1% osmium tetroxide in 0.1 M sodium cacodylate for 1 h. After the fixation step, the biofilms were dehydrated in ethanol (30, 50, 70, 90%, and absolute alcohol) and dried. The biofilms were then examined using the SEM JSM-6390LV scanning electron microscope (Jeol, Tokyo, Japan) operated at 15 kV.

Statistical analysis

The statistical analyses were made using the SPSS v. 22.0 (IBM, Amonk, NY, USA) software. The distributions of the results of the broth microdilution, MBC_{100} determination, biofilm formation and interference assays were verified using the D'Agostino–Pearson test, and the comparisons of the AgNP-treated and AgNP-not treated bacteria and of the different AgNPs concentration results were made using the *t*-test and the one-way ANOVA ($p < 0.05$).

RESULTS

Characterization of the AgNPs

The AgNPs used in this study were spherical, and presented a zeta potential of -31.7 ± 2.8 mV. They were also characterized by a 0.231 polydispersity, and sizes of 28.0 ± 13.1 nm. These results confirmed what was previously described for these AgNPs (*Stanisic et al., 2018*).

Detection of biofilm formation by *C. pseudotuberculosis* strains

A total of eight *C. pseudotuberculosis* isolates that were used in this study were classified as biofilm formers. The OD_{595} of the negative control was 0.136, and OD_{595} values between 0.136 and 0.272 determined the strains that were poor biofilm producers. If the OD_{595} was between 0.272 and 0.544, the *C. pseudotuberculosis* strain was considered as an isolate with moderate biofilm production activity, and $OD_{595} > 0.544$ characterized the strain as a strong biofilm producer (*Nostro et al., 2007*). In this experiment, strains 1002 and T1 were characterized as poor biofilm producers. Strains N1 and CAPJ4, and clinical isolates 06 and 96, were characterized as moderate biofilm producers, while the clinical isolates 05 and 15 were considered as strong biofilm producers (Fig. 1).

Antimicrobial susceptibility assessment of planktonic and biofilm cells of *C. pseudotuberculosis*

The evaluation of the antimicrobial activity of AgNP against *C. pseudotuberculosis* using the broth microdilution methodology demonstrated a growth inhibition of most isolates at a concentration of 0.156 mg/mL, with the lowest MIC_{100} being 0.08 mg/mL. Similar

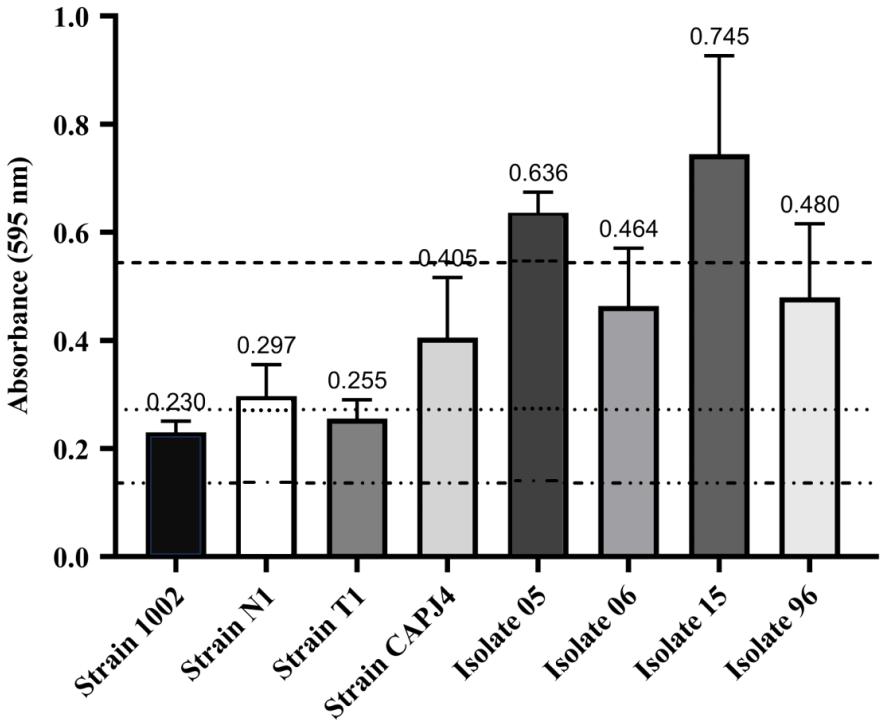

Figure 1 Biofilm formation by *Corynebacterium pseudotuberculosis* reference strains and clinical isolates. Bars indicate the standard deviations. The dashed lines indicate the mean value of the negative control ($OD_{595} = 0.136$), weak biofilm production (OD_{595} between 0.136 and 0.272), moderate biofilm production (OD_{595} between 0.272 and 0.544) and strong biofilm production ($OD_{595} > 0.544$). The results express the means of three independent experiments.

Full-size DOI: 10.7717/peerj.16751/fig-1

results were observed among the reference strains for the bactericidal action of AgNPs, with MBC_{100} values equivalent to 0.156 mg/mL. AgNPs had a lower bactericidal action among clinical isolates (Table 1). A MIC_{100} curve was created to visualize the antibacterial action of the AgNPs at different concentrations (Fig. S1).

The evaluation of the action of the AgNPs in consolidated biofilms was measured at three incubation periods: 0 h, 24 h and 48 h. After adding the AgNP colloidal solution to the consolidated biofilms, all bacteria showed biofilm reductions at 24 h and 48 h of incubation and at the different tested concentrations. The greatest decreases were observed for the consolidated biofilms of the clinical isolates, except for isolate 06, and the CAPJ4 strain. The consolidated biofilms from strains 1002, N1, and T1 were less sensitive to the action of AgNPs (Fig. 2).

The interference on biofilm formation assay showed that, within 48 h of incubation, the AgNPs were able to significantly interfere with the formation of biofilm by the bacterial strains, with interference values greater than 80% at a AgNP concentration of 4 mg/mL for the reference strains N1 and CAPJ4. The percentages of interference in biofilm formation by the AgNPs are shown in Table 2. The AgNPs were able to prevent biofilm formation

Table 1 Sensitivity profile of *C. pseudotuberculosis* reference strains and clinical isolates to AgNPs.

Strains of *C. pseudotuberculosis*	MIC_{100} (mg/mL)	MBC_{100} (mg/mL)
1002	0.156	0.156
N1	0.156	0.156
T1	0.156	0.156
CAPJ4	0.08	0.156
Isolate 05	0.312	0.312
Isolate 06	0.156	0.312
Isolate 15	0.08	0.312
Isolate 96	0.156	0.312

Notes.
The results express the means of three different experiments.
MIC_{100}, minimum AgNP concentration capable to inhibit 100% of the bacterial growth; MBC_{100}, minimum AgNP concentration capable to kill all the bacteria.

by the reference strains at all concentrations tested. Also, a significant reduction in biofilm formation was observed in all clinical isolates at the concentrations tested herein (Fig. 3).

Scanning electron microscopy

SEM micrographs obtained from AgNP-treated and AgNP-not treated *C. pseudotuberculosis* are shown in Figs. 4A and 4B. Untreated *C. pseudotuberculosis* was typically presented as cocci or coccobacilli, with a smooth, intact cell wall, covered by an amorphous exopolysaccharide matrix.

After the exposure to the AgNP colloidal solution (4 mg/mL) for 48 h, the amount of *C. pseudotuberculosis* biofilm significantly reduced (Fig. 4C), with a large quantity of debris and materials deposited on the bacterial surface (Fig. 4D), and even a complete disruption of the bacterial biofilm, with apparent loss of adhesion (Fig. 4E). Some bacteria that remained intact presented surface vesicles (Fig. 4F), indicating an increased plasma membrane permeability and the release of intracellular components.

DISCUSSION

C. pseudotuberculosis is the etiological agent of CL, a disease that causes a significant reduction in the productivity and in the reproductive efficiency of infected animals, leading to economic losses (*Costa et al., 2022*). In addition, the treatment of the disease is generally refractory to antibiotic therapy. With the objective to develop new therapeutical options for CL, we identified that *Fusarium oxysporum*-based AgNPs can be a promising antimicrobial agent, because of its marked antibacterial action on *C. pseudotuberculosis* planktonic cells and on its associated biofilm.

Semi-quantitative analysis are valid tools to determine the capacity of biofilm formation, and it has been described that many bacterial isolates do not produce or are poor biofilm producers, and this fact is correlated with different sensitivities to antimicrobial agents (*Sá et al., 2013*). Considering this situation, we included in our study different *C. pseudotuberculosis* reference strains and clinical isolates, which showed distinct biofilm production capacities. Interestingly, the CAPJ4 strain was recently used as a reference for

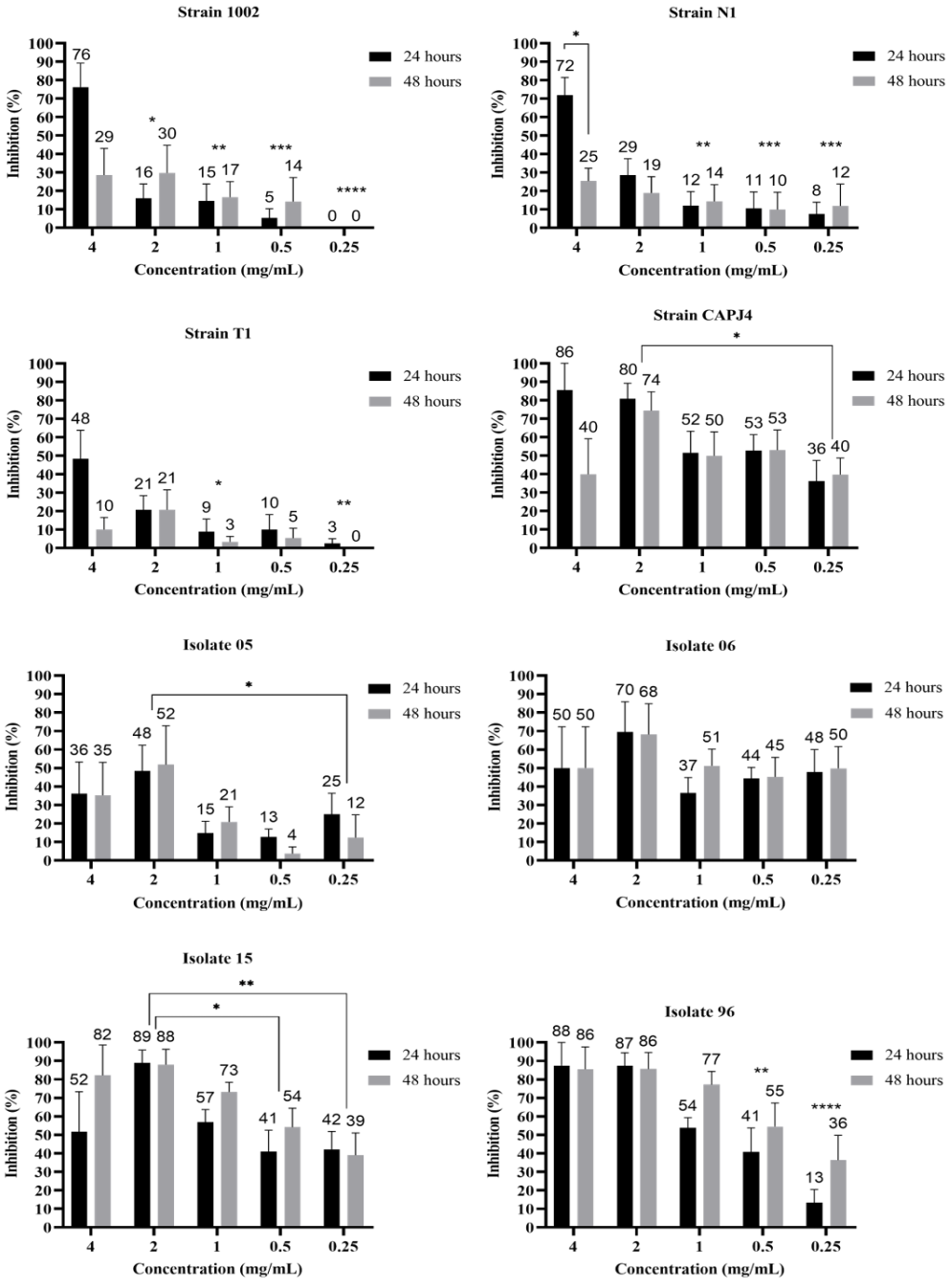

Figure 2 AgNP activity on consolidated biofilms of *C. pseudotuberculosis* reference strains and clinical isolates after 24 and 48 hours of treatment. Results express the inhibition means (in %) from three independent experiments. The bars represent the standard deviations. Asterisks indicate statistical differences between bacterial cells treated with different concentrations of AgNP and the not-treated control, at different times, analyzed using analysis of variance (one-way ANOVA) and the *t*-test. $^{*}p < 0.03$, $^{**}p < 0.005$, $^{***}p < 0.0009$ and $^{****}p < 0.0001$.

Full-size DOI: 10.7717/peerj.16751/fig-2

Table 2 AgNP interference in *C. pseudotuberculosis* biofilm formation. The results express the percentage of inhibition ± standard deviation (confidence interval of 95%) of biofilm formation after 48 h of incubation with AgNPs, as means of three independent experiments.

Strain of *C. pseudotuberculosis*	AgNP (mg/mL)				
	4	**2**	**1**	**0.5**	**0.25**
1002	78 ± 19 (57–99)	53 ±29 (22–84)	42 ± 17 (23–60)	68 ±20 (47–89)	52 ± 23 (27–76)
N1	86 ± 16 (69–100)	65 ± 24 (39–91)	49 ± 17 (33–64)	59 ± 17 (41–77)	68 ± 12 (55–81)
T1	75 ± 34 (40–100)	84 ± 8 (76–93)	66 ± 16 (49–82)	87 ±10 (77–97)	62 ± 17 (44–80)
CAPJ4	91 ± 11 (80–100)	86 ± 12 (73–99)	83 ± 10 (73–94)	90 ± 5 (85–95)	89 ± 4 (84–93)
Isolate 05	59 ±22 (36–83)	71 ± 14 (55–86)	71 ± 8 (62–80)	80 ± 9 (70–91)	79 ± 9 (70–89)
Isolate 06	66 ± 29 (36–97)	79 ± 6 (72–86)	59 ± 20 (38–61)	79 ± 11 (67–91)	81 ± 8 (72–89)
Isolate 15	73 ±18 (54–93)	79 ± 12 (63–89)	77 ± 4 (73–81)	89 ± 4 (85–93)	88 ± 4 (83–92)
Isolate 96	78 ± 9 (68–87)	83 ± 12 (7–95)	83 ± 7 (75–90)	88 ± 6 (82–94)	87 ± 6 (81–93)

Notes.
SD, Standard Deviation; CI 95%, confidence intervals.

a proteomic analysis focused on its virulence and capacity of biofilm production, and exhibited a marked up-regulation of the galactose-1-phosphate uridylyltransferase and N-acetylmuramoyl-L-alanine amidase enzymes, which are involved in biofilm formation and exopolysaccharide biosynthesis (*De Sá et al., 2021*).

Based on global metabolomic profiles, bacteria with weak and strong biofilm formation capacities present themselves as two distinct groups. Bacteria that are classified as poor biofilm producers can express more metabolites than bacteria with strong biofilm production; this situation indicates a higher endogenous metabolic activity (especially lipid metabolism), on which some isolates show a greater tendency to remain in their planktonic and free-floating state, than bacteria with strong biofilm production (*Wong et al., 2018*). Such results may justify the distinct profiles of biofilm production among *C. pseudotuberculosis* isolates. In addition, bacteria with weak to strong adherent biofilms can present multidrug resistant phenotypes and this characteristic can play a vital role in pathological processes based on the bacterial resistance to the host immunological system, and to antimicrobial agents (*Diriba et al., 2020*).

The results of the sensitivity test using the broth microdilution methodology demonstrated the effectiveness of AgNPs to inhibit the growth and in the inactivation of *C. pseudotuberculosis* reference strains and clinical isolates. This result agrees with studies showing the antibacterial activity of AgNPs obtained by green synthesis methods against *E. coli*, *Klebsiella pneumoniae*, *Salmonella* Typhimurium and *Salmonella* Enteritidis (*Loo et al., 2018*). *Punjabi et al. (2018)* concluded that AgNPs obtained by an extracellular synthesis methodology using *Pseudomonas hibiscicola* showed high efficiency against multi-drug-resistant (MDR) clinical isolates of methicillin-resistant *Staphylococcus aureus* (MRSA), extended spectrum β lactamases (ESBL) producer *K. pneumoniae*, vancomycin-resistant *Enterococcus faecalis* (VRE), and *M. tuberculosis*, with MICs ranging from 0.6–1.5 mg/mL; the results obtained by these authors showed the antimicrobial potential of AgNPs against resistant bacterial strains isolated from human hospitals. Bacterial inhibition tests also show that the effectiveness of AgNPs is dependent on size and shape, with spherical and

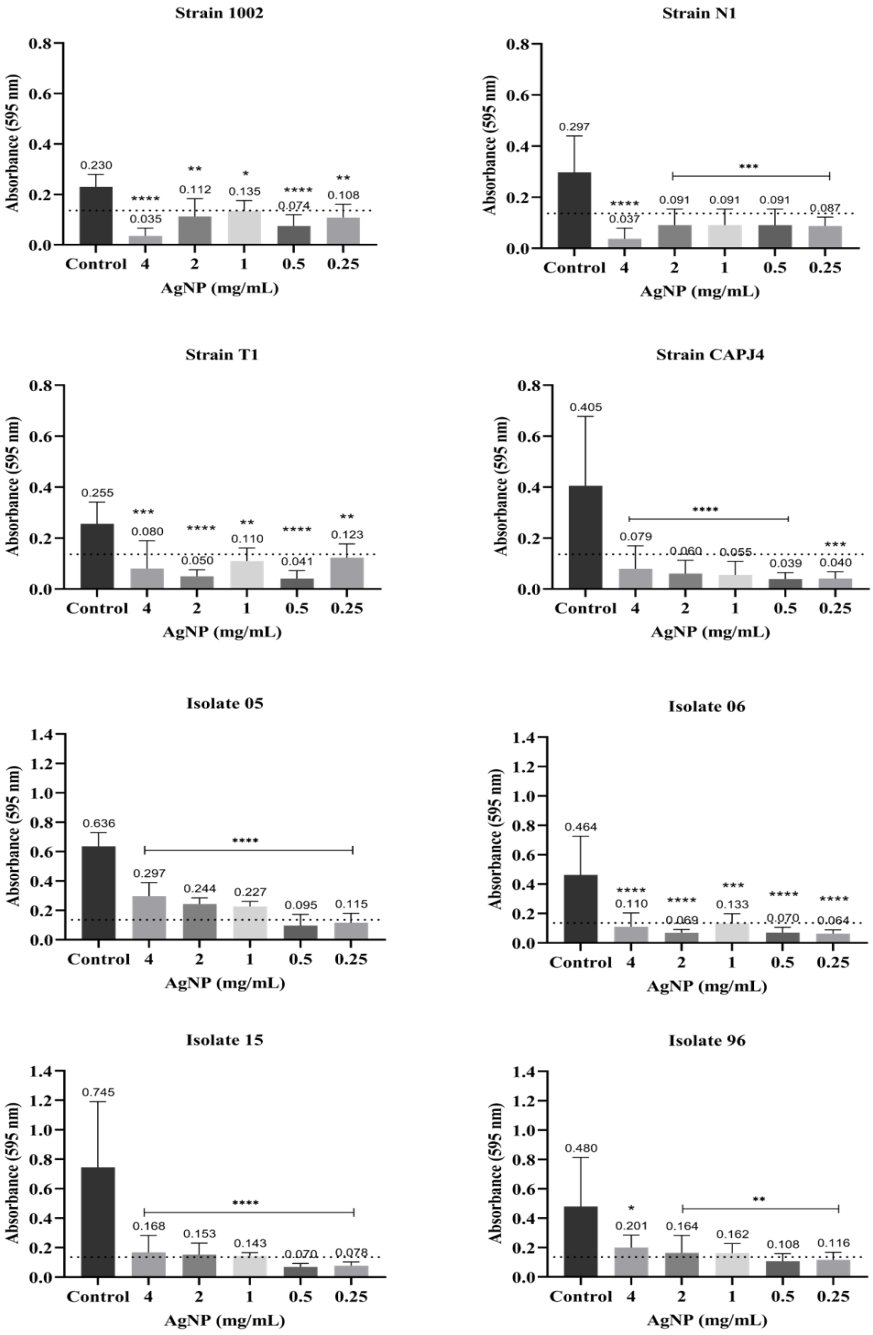

Figure 3 AgNP interference in the biofilm formation by *C. pseudotuberculosis* reference strains and clinical isolates. Bars represent standard deviations. The dashed line indicates the mean value of the negative control ($OD_{595} = 0.136$). Asterisks indicate statistical differences between bacterial cells not treated and treated with different concentrations of nanoparticles, analyzed using analysis of variance (one-way ANOVA). $^{*}p < 0.05$; $^{**}p < 0.005$; $^{***}p < 0.0003$; $^{****}p < 0.0001$.

Full-size DOI: 10.7717/peerj.16751/fig-3

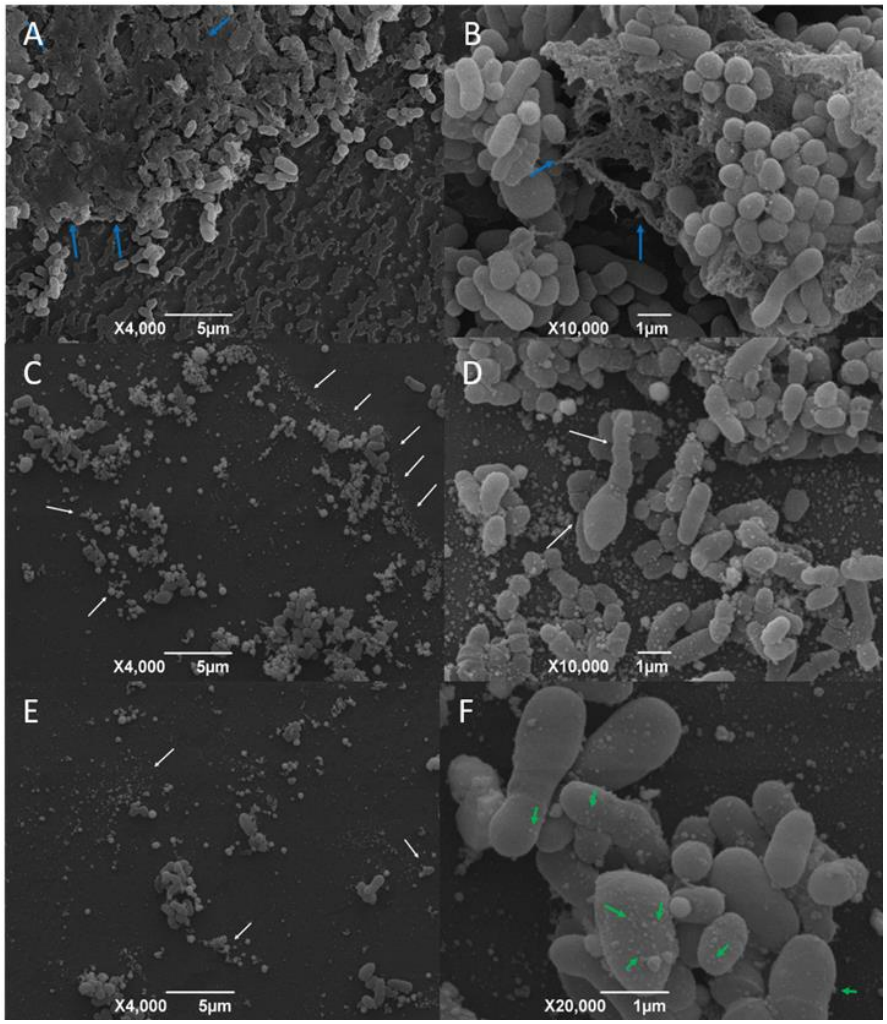

Figure 4 Representative scanning electron micrographs of the structure of mature *C. pseudotuberculosis* biofilms untreated (A and B) and treated with AgNPs at the concentration of 4 mg/mL (C, D, E and F). Blue arrows indicate the presence of an exopolysaccharide matrix in the mature biofilm. White arrows indicate cell deformities and debris. Green arrows point to the presence of vesicles on the bacterial surface.
Full-size DOI: 10.7717/peerj.16751/fig-4

smaller AgNPs being more efficient (*Raza et al., 2016*), like the nanoparticles used against *C. pseudotuberculosis* herein.

Few studies report the action of antimicrobials on *C. pseudotuberculosis* biofilm. *Sá et al. (2013)* analyzed the effectiveness of disinfectants in interfering with *C. pseudotuberculosis* biofilm formation and in the consolidated biofilm, and they found that disinfectants were not effective against the consolidated biofilm; however, they observed that iodine inhibited the biofilm formation in 33% of the bacterial isolates, and quaternary ammonia was able to prevent the biofilm formation by 28% of isolates. It is noteworthy that the consolidation of a biofilm is a part of the attachment process, when there is a formed exopolymer that connects the bacteria between themselves and with the surface (*Garrett, Bhakoo &*

Zhang, 2008). Our study is the first one that evaluated the action of nanoparticles on *C. pseudotuberculosis* biofilm. However, the antibiofilm mechanisms of silver nanoparticles are not fully known, and can be dependent on the nanoparticle physicochemical properties and on the type of microorganism (*Durán et al., 2016*).

The results of the present study indicated that the consolidated biofilms of *C. pseudotuberculosis* suffered the action of AgNP at different concentrations. Natural compounds, such as extracellular fungal compounds, may be more effective stabilizing agents, since they prevent particle aggregation and enhance the antimicrobial activity of AgNPs, increasing bacterial inactivation in the biofilm and reducing nanoparticle cytotoxicity (*Liu et al., 2019*). The same AgNPs used in our study were administered as an ointment (with an AgNP concentration of 2.56 mg/mL) to sheep and goats with surgical wounds, and induced an accelerated wound healing process, in the absence of any clinical sign of toxicity and without any influence on hematological and clinical biochemistry parameters that could indicate a toxigenic process induced by the AgNPs (*Santos et al., 2019*). According to *Estevez et al. (2020)*, AgNPs produced with extracellular extracts of *Phanerochaete chrysosporium* cells (PchNPs) exhibited an activity based on the eradication of *E. coli* and *C. albicans* biofilms. *Siddique et al. (2020)* concluded that the percentage of biofilm inhibition by AgNPs in *K. pneumoniae* MDR strain MF953600 was 64%, and 84% for the MF953599 strain at the concentration of 100 mg/mL. The production of the exopolymer substance decreased after the AgNP treatment, while cellular protein leakage increased due to higher rates of cell membrane disruption. Size, shape, surface, and interior properties of nanoparticles (NPs) are important factors to be considered in biofilm control (*Liu et al., 2019*). The size of NPs is a crucial factor to be considered regarding its penetration into biofilms and should not exceed the dimensions of water channels in these biofilms. As the sizes of water channels in biofilms are difficult to estimate, the ideal size of NPs that can present a significant activity in biofilms should range between 5 and 100–200 nm (*Peulen & Wilkinson, 2011*), and the AgNPs used in this study presented sizes of 28 .0 $\pm$ 13.1 nm. On the other hand, the reduced sensitivity of some consolidated *C. pseudotuberculosis* biofilms may be related to a lower diffusion and adsorption of the antimicrobial into the exopolymer matrix, which only allows the transport of nutrients and residual metabolites through the water channels and hinders the transport of antimicrobial agents. Considering this situation, only the bacteria present on the surface of the biofilm can be affected (*Koo et al., 2017*).

The difference in the action of AgNPs in biofilms of reference strains and clinical isolates can be attributed to the constant maintenance of the reference strains in the culture media used in the experiments. *Djais et al. (2019)*, who evaluated the effect of propolis extract in the formation of biofilm by *Streptococcus mutans*, describe that this situation can be a consequence of the sucrose and other polysaccharides present in the TSB medium. Sucrose is used by oral streptococci to produce extracellular polysaccharides present in dental biofilms. Glucans are essential for dental plaque formation and increase the attachment of bacteria to the tooth surface, and it is known that fructan can enhance the biofilm virulence, since it is a binding site for *S. mutans* adhesion (*Djais et al., 2019*).

The biofilm formation interference test is one of the strategies adopted to control the stages of biofilm development. The objective of the interference test is to inhibit the initial fixation of bacteria on biofilm-forming surfaces, thus reducing the chances of biofilm development (*Subhadra et al., 2018*). Biofilm formation control strategies have been widely used in the biomedical field, such as the use of antibiotic-coated catheters (*Balne et al., 2018*), or even materials with superhydrophobic textures thar are able to induce a delayed adhesion and inhibit the production of bacterial biofilm (*Falde et al., 2016*). The inhibition of the initial biofilm fixation by biomaterials is also a useful strategy for controlling biofilm formation. The biogenic AgNPs in the present study proved to be efficient not only in preventing bacterial growth, but significantly reduced biofilm formation in all *C. pseudotuberculosis* isolates; this situation is very pertinent, since the formation of biofilm by this specific bacterium is usually correlated with its virulence and with its capacity to induce a chronic disease (*Dorella et al., 2006*).

The initial attachment of cells to biofilm-forming surfaces occurs within the first two days of biofilm formation (*Subhadra et al., 2018*). AgNPs acted for 48 h in *C. pseudotuberculosis*, controlling the change between planktonic and biofilm-associated forms. This control was also observed in Gram-positive cocci treated with small molecules known as aryl rhodanines (*Opperman et al., 2009*), and in *Vibrio cholerae* treated with di-Cyclic GMP inhibitors (*Connera et al., 2017*). *Saising et al. (2012)* found that galidermin was able to completely inhibit biofilm formation at concentrations of 4 to 8 μg/mL; these authors also describe that the levels of transcription of the *atl* genes, which encode molecules that participates in the primary adhesion, and *ica* genes, which encodes an adhesin related to exopolysaccharide production, were significantly reduced in the presence of the antimicrobial agent. Antimicrobial peptides are also known to interfere with biofilm formation by different bacterial pathogens. Antibiofilm peptide 1018 blocked ppGpp, which is known to play an important role in biofilm formation, and the treatment with this peptide completely prevented biofilm formation and led to the eradication of mature biofilms formed by *P. aeruginosa*, *E. coli*, *Acinetobacter baumannii*, *K. pneumoniae*, methicillin resistant *S. aureus*, *Salmonella* Typhimurium and *Burkholderia cenocepacia* (*Fuente-Núñez et al., 2014*).

As a confirmation of the biofilm formation using a 96-well culture plate, we examined the formed biofilms by scanning electron microscopy. According to our results, the *C. pseudotuberculosis* strains demonstrated an ability to form mature biofilms. These results are in accordance with a previous study that observed the biofilm formation and consolidation by the *C. pseudotuberculosis* CAPJ4 strain (*De Sá et al., 2021*). We were able to observe that AgNP-treated *C. pseudotuberculosis* biofilms showed severe cell destruction and biofilm disruption. As described by other authors, the bacterial exposure to other types of AgNPs resulted in the adhesion of nanoparticles on the cell wall and membrane, causing significant morphological changes, such as cytoplasm shrinkage, membrane displacement and cell disruption (*Dakal et al., 2016*). SEM images of *P. aeruginosa* biofilm showed few bacterial aggregates and fewer viable bacteria after 24 h of exposure to nanoparticles (*Mu et al., 2016*). The 3 h treatment of *S. aureus* biofilm with catechin-copper nanoparticles dramatically changed the shape and size of the cells, resulting in wrinkled cell walls and

in the adhesion of many materials on the bacterial surface (*Li et al., 2015*), a result very similar to what was found in our images. The formation of vesicles on the cell surface of *C. pseudotuberculosis* is consistent with an increased cytoplasmic membrane permeability and leakage of cellular compounds (*Diao et al., 2004*). A similar result was found after exposure of *P. aeruginosa* to ozone (*Zhang et al., 2011*). Increased cytoplasmic membrane permeability and destabilization of cell structures and biomolecules are common AgNP and ozone mechanisms of action (*Habash et al., 2014*; *Singh et al., 2015*; *Dakal et al., 2016*).

CONCLUSIONS

The *Fusarium oxysporum*-based biogenic AgNPs showed to be significantly effective against *C. pseudotuberculosis* in the planktonic form. Our study is the first to describe the action of nanoparticles on *C. pseudotuberculosis* biofilms and our findings indicate a high efficacy regarding the ability to cause biofilm disruption and destruction, with significant bacterial morphological changes. The use of biologically synthesized AgNPs represented an adequate strategy for biofilm formation interference. In this way, biogenic silver nanoparticles can be seen as promising antimicrobial agents for the control of caseous lymphadenitis in small ruminants.

ACKNOWLEDGEMENTS

The authors give thanks to the Electronic Microscopy Unit of the Instituto Gonçalo Moniz, (FIOCRUZ/Bahia) for the use of the scanning electron microscope, and to Francisca Soares (LABIMUNO ICS/UFBA) for technical assistance.

ADDITIONAL INFORMATION AND DECLARATIONS

Funding

This study was funded by the Fundação de Apoio à Pesquisa e Extensão (FAPEX), through continuous resources obtained by extension projects. Laerte Marlon Santos and Mauricio Alcantara Kalil are PhD fellows from the Coordenação de Aperfeiçoamento de Pessoal de Nível Superior (CAPES). Ricardo Wagner Portela is a Technical Development fellow from the Conselho Nacional de Desenvolvimento Científico (CNPQ—Proc. 310058/2022-8). The funders had no role in study design, data collection and analysis, decision to publish, or preparation of the manuscript.

Grant Disclosures

The following grant information was disclosed by the authors:
Fundação de Apoio à Pesquisa e Extensão (FAPEX), through continuous resources obtained by extension projects.
Laerte Marlon Santos and Mauricio Alcantara Kalil are PhD fellows from the Coordenação de Aperfeiçoamento de Pessoal de Nível Superior (CAPES).
Ricardo Wagner Portela is a Technical Development fellow from the Conselho Nacional de Desenvolvimento Científico: CNPQ—Proc. 310058/2022-8.

Competing Interests

Vasco Azevedo and Debmalya Barh are Academic Editors for PeerJ.

Author Contributions

- Laerte Marlon Santos conceived and designed the experiments, performed the experiments, prepared figures and/or tables, and approved the final draft.
- Daniela Méria Rodrigues performed the experiments, prepared figures and/or tables, and approved the final draft.
- Bianca Vilas Boas Alves performed the experiments, prepared figures and/or tables, and approved the final draft.
- Mauricio Alcântara Kalil performed the experiments, prepared figures and/or tables, and approved the final draft.
- Vasco Azevedo analyzed the data, authored or reviewed drafts of the article, and approved the final draft.
- Debmalya Barh analyzed the data, authored or reviewed drafts of the article, and approved the final draft.
- Roberto Meyer conceived and designed the experiments, analyzed the data, authored or reviewed drafts of the article, and approved the final draft.
- Nelson Duran conceived and designed the experiments, analyzed the data, authored or reviewed drafts of the article, and approved the final draft.
- Ljubica Tasic conceived and designed the experiments, authored or reviewed drafts of the article, and approved the final draft.
- Ricardo Wagner Portela conceived and designed the experiments, prepared figures and/or tables, authored or reviewed drafts of the article, and approved the final draft.

Data Availability

The following information was supplied regarding data availability:

All the raw data is available in the Supplemental Files.

Supplemental Information

Supplemental information for this article can be found online at http://dx.doi.org/10.7717/peerj.16751#supplemental-information.

REFERENCES

Almeida S, Dorneles EMS, Diniz C, Abreu V, Sousa C, Alves J, Carneiro A, Bagano P, Spier S, Barh D, Lage AP, Figueiredo H, Azevedo V. 2017. Quadruplex PCR assay for identification of *Corynebacterium pseudotuberculosis* differentiating biovar Ovis and Equi. *BMC Veterinary Research* **13**:290 DOI 10.1186/s12917-017-1210-5.

Ballottin D, Fulaz S, Cabrini F, Tsukamoto J, Durán N, Alves OL, Tasic L. 2017. Antimicrobial textiles: biogenic silver nanoparticles against *Candida* and *Xanthomonas*. *Materials Science and Engineering: C* **75**:582–589 DOI 10.1016/j.msec.2017.02.110.

Balne PK, Harini S, Dhand C, Dwivedi N, Chalasani MLS, Verma NK, Barathi VA, Beuerman R, Agrawal R, Lakshminarayanan R. 2018. Surface characteristics and antimicrobial properties of modified catheter surfaces by polypyrogallol and metal ions. *Materials Science and Engineering: C* **90**:673–684 DOI 10.1016/j.msec.2018.04.095.

Barral TD, Kalil MA, Mariutti RB, Arni RK, Gismene C, Sousa FS, Collares T, Seixas FK, Borsuk S, Estrela-Lima A, Azevedo V, Meyer R, Portela RW. 2022. Immunoprophylactic properties of the *Corynebacterium pseudotuberculosis*-derived MBP:PLD:CP40 fusion protein. *Applied Microbiology and Biotechnology* **106**:8035–8051 DOI 10.1007/s00253-022-12279-1.

Bastos BL, Portela RWD, Dorella FA, Ribeiro D, Seyffert N, Castro TL, Miyoshi A, Oliveira SC, Meyer R, Azevedo V. 2012. Corynebacterium *pseudotuberculosis*: immunological responses in animal models and zoonotic potential. *Journal of Clinical and Cellular Immunology* **S4**:005 DOI 10.4172/2155-9899.S4-005.

Connera JG, Zamorano-Sánchez D, Park JH, Sondermann H, Yildiz FH. 2017. The ins and outs of cyclic di-GMP signaling in *Vibrio cholerae*. *Current Opinion in Microbiology* **36**:20–29 DOI 10.1016/j.mib.2017.01.002.

Costa JO, Barral TD, Portela RD, Da Costa LNF, Bittencourt CN, Machado AL, Marques FS, Cavalcante AKDS. 2022. Correlation between the natural infection by *Corynebacterium pseudotuberculosis* in goats and serum progesterone levels and corpus luteum development. *Domestic Animal Endocrinology* **78**:106677 DOI 10.1016/j.domaniend.2021.106677.

Dakal TC, Kumar A, Majumdar RS, Yadav V. 2016. Mechanistic basis of antimicrobial actions of silver nanoparticles. *Frontiers in Microbiology* **7**:1831 DOI 10.3389/fmicb.2016.01831.

De Oliveira A, Cataneli Pereira V, Pinheiro L, Moraes Riboli DF, Benini Martins K, Ribeiro de Souza da Cunha ML. 2016. Antimicrobial resistance profile of planktonic and biofilm cells of *Staphylococcus aureus* and coagulase-negative Staphylococci. *International Journal of Molecular Sciences* **17**:1423 DOI 10.3390/ijms17091423.

De Sá MCA, Da Silva WM, Rodrigues CCS, Rezende CP, Marchioro SB, Rocha Filho JTR, Sousa TJ, De Oliveira HP, Da Costa MM, Figueiredo HCP, Portela RD, Castro TLP, Azevedo V, Seyffert N, Meyer R. 2021. Comparative proteomic analyses between biofilm-forming and non-biofilm-forming strains of *Corynebacterium pseudotuberculosis* isolated from goats. *Frontiers in Veterinary Science* **8**:614011 DOI 10.3389/fvets.2021.614011.

Diao H, Li X, Gu J, Shi H, Xie Z. 2004. Electron microscopic investigation of the bactericidal action of electrochemical disinfection in comparison with chlorination, ozonation and Fenton reaction. *Process Biochemistry* **39**:1421–1426 DOI 10.1016/S0032-9592(03)00274-7.

Diriba K, Kassa T, Alemu Y, Bekele S. 2020. *In vitro* biofilm formation and antibiotic susceptibility patterns of bacteria from suspected external eye infected patients attending ophthalmology clinic, Southwest Ethiopia. *International Journal of Microbiology* **2020**:8472395 DOI 10.1155/2020/8472395.

Djais AA, Putri N, Putri AR, Darwita RR, Bachtiar BM. 2019. Effect of propolis on *Streptococcus mutans* biofilm formation. *Pesquisa Brasileira em Odontopediatria e Clínica Integrada* **19**:e5221 DOI 10.4034/PBOCI.2019.191.138.

Dorella FA, Pacheco LG, Oliveira SC, Miyoshi A, Azevedo V. 2006. *Corynebacterium pseudotuberculosis*: microbiology, biochemical properties, pathogenesis and molecular studies of virulence. *Veterinary Research* **37**:201–218 DOI 10.1051/vetres:2005056.

Durán N, Durán M, De Jesus MB, Seabra AB, Fávaro WJ, Nakazato G. 2016. Silver nanoparticles: a new view on mechanistic aspects on antimicrobial activity. *Nanomedicine* **12**:789–799 DOI 10.1016/j.nano.2015.11.016.

Estevez MB, Raffaelli S, Mitchell SG, Faccio R, Alborés S. 2020. Biofilm eradication using biogenic silver nanoparticles. *Molecules* **25**:2023 DOI 10.3390/molecules25092023.

Falde EJ, Yohe ST, Colson YL, Grinstaff MW. 2016. Superhydrophobic materials for biomedical applications. *Biomaterials* **104**:87–103 DOI 10.1016/j.biomaterials.2016.06.050.

Fernandez CC, Sokolonski AR, Fonseca MS, Stanisic D, Araújo DB, Azevedo V, Portela RD, Tasic L. 2021. Applications of silver nanoparticles in dentistry: advances and technological innovation. *International Journal of Molecular Sciences* **22**:2485 DOI 10.3390/ijms22052485.

Fonseca MS, Deegan KR, Tomé LM, Mendonça MA, Sokolonski AR, Gondim LQ, Azevedo V, Meyer R, Tasic L, Góes-Neto A, Portela RW. 2023. First description of *Candida haemulonii* infecting a snake *Boa constrictor*: molecular, pathological and antifungal sensitivity characteristics. *Microbial Pathogenesis* **180**:106164 DOI 10.1016/j.micpath.2023.106164.

Fonseca MS, Rodrigues DM, Sokolonski AR, Stanisic D, Tomé LM, Góes-Neto A, Azevedo V, Meyer R, Araújo DB, Tasic L, Portela RD. 2022. Activity of *Fusarium oxysporum*-based silver nanoparticles on *Candida* spp. oral isolates. *Nanomaterials* **12**:501 DOI 10.3390/nano12030501.

Fontaine MC, Baird GJ. 2008. Caseous lymphadenitis. *Small Ruminant Research* **76**:42–48 DOI 10.1016/j.smallrumres.2007.12.025.

Fuente-Núñez C de la, Reffuveille F, Haney EF, Straus SK, Hancock REW. 2014. Broad-spectrum anti-biofilm peptide that targets a cellular stress response. *PLOS Pathogens* **10**:e1004152 DOI 10.1371/journal.ppat.1004152.

Garrett TC, Bhakoo M, Zhang Z. 2008. Bacterial adhesion and biofilms on surfaces. *Progress in Natural Science* **18**:1049–1056 DOI 10.1016/j.pnsc.2008.04.001.

Guedes MT, Souza BC, Sousa TJ, Loureiro D, Moura-Costa LF, Azevedo V, Meyer R, Portela RW. 2015. Infecção por *Corynebacterium pseudotuberculosis* em equinos: aspectos microbiológicos, clínicos e preventivos. *Pesquisa Veterinaria Brasileira* **35**:701–708 DOI 10.1590/s0100-736x2015000800001.

Habash MB, Park AJ, Vis EC, Harris RJ, Khursigara CM. 2014. Synergy of silver nanoparticles and aztreonam against *Pseudomonas aeruginosa* PAO1 biofilms. *Antimicrobial Agents and Chemotherapy* **58**:5818–5830 DOI 10.1128/AAC.03170-14.

Kalil MA, Santos LM, Barral TD, Rodrigues DM, Pereira NP, Sá M da CA, Umsza-Guez MA, Machado BAS, Meyer R, Portela RW. 2019. Brazilian green propolis as a therapeutic agent for the post-surgical treatment of caseous lymphadenitis in sheep. *Frontiers in Veterinary Science* **6**:1–10 DOI 10.3389/fvets.2019.00399.

Koo H, Allan RN, Howlin RP, Stoodley P, Hall-Stoodley L. 2017. Targeting microbial biofilms: current and prospective therapeutic strategies. *Nature Reviews Microbiology* **15**:740–755 DOI 10.1038/nrmicro.2017.99.

Li H, Chen Q, Zhao J, Urmila K. 2015. Enhancing the antimicrobial activity of natural extraction using the synthetic ultrasmall metal nanoparticles. *Scientific Reports* **5**:11033 DOI 10.1038/srep11033.

Liu Y, Shi L, Su L, Van der Mei HC, Jutte PC, Ren Y, Busscher HJ. 2019. Nanotechnology-based antimicrobials and delivery systems for biofilm-infection control. *Chemical Society Reviews* **48**:428–446 DOI 10.1039/c7cs00807d.

Loo YY, Rukayadi Y, Nor-Khaizura MA, Kuan CH, Chieng BW, Nishibuchi M, Radu S. 2018. *In vitro* antimicrobial activity of green synthesized silver nanoparticles against selected Gram-negative foodborne pathogens. *Frontiers in Microbiology* **9**:1555 DOI 10.3389/fmicb.2018.01555.

Loureiro D, Portela RW, Sousa TJ, Rocha F, Pereira FL, Dorella FA, Carvalho AF, Menezes N, Macedo ES, Moura-Costa LF, Meyer R, Leal CA, Figueiredo HC, Azevedo V. 2016. Complete genome sequence of *Corynebacterium pseudotuberculosis* viscerotropic strain N1. *Genome Announcements* **4**:e01673-15 DOI 10.1128/genomeA.01673-15.

Macià MD, Rojo-Molinero E, Oliver A. 2014. Antimicrobial susceptibility testing in biofilm-growing bacteria. *Clinical Microbiology and Infection* **20**:981–990 DOI 10.1111/1469-0691.12651.

Mariano DC, Sousa Tde J, Pereira FL, Aburjaile F, Barh D, Rocha F, Pinto AC, Hassan SS, Saraiva TD, Dorella FA, De Carvalho AF, Leal CA, Figueiredo HC, Silva A, Ramos RT, Azevedo VA. 2016. Whole-genome optical mapping reveals a mis-assembly between two rRNA operons of *Corynebacterium pseudotuberculosis* strain 1002. *BMC Genomics* **17**:315 DOI 10.1186/s12864-016-2673-7.

Moura-Costa LF, Bahia RC, Carminati R, Vale VL, Paule BJ, Portela RW, Freire SM, Nascimento I, Schaer R, Barreto LM, Meyer R. 2008. Evaluation of the humoral and cellular immune response to different antigens of *Corynebacterium pseudotuberculosis* in Canindé goats and their potential protection against caseous lymphadenitis. *Veterinary Immunology and Immunopathology* **126**:131–141 DOI 10.1016/j.vetimm.2008.06.013.

Mu H, Tang J, Liu Q, Sun C, Wang T, Duan J. 2016. Potent antibacterial nanoparticles against biofilm and intracellular bacteria. *Scientific Reports* **6**:18877 DOI 10.1038/srep18877.

Norman TE, Batista M, Lawhon SD, Zhang S, Kuskie KR, Swinford AK, Bernstein LR, Cohen ND. 2014. *In vitro* susceptibility of equine-obtained isolates of *Corynebacterium pseudotuberculosis* to gallium maltolate and 20 other antimicrobial agents. *Journal of Clinical Microbiology* **52**:2684–2685 DOI 10.1128/JCM.01252-14.

Nostro A, Roccaro AS, Bisignano G, Marino A, Cannatelli MA, Pizzimenti FC, Cioni PL, Procopio F, Blanco AR. 2007. Effects of oregano, carvacrol and thymol on *Staphylococcus aureus* and *Staphylococcus epidermidis* biofilms. *Journal of Medical Microbiology* **56**:519–523 DOI 10.1099/jmm.0.46804-0.

Opperman TJ, Kwasny SM, Williams JD, Khan AR, Peet NP, Moir DT, Bowlin TL. 2009. Aryl rhodanines specifically inhibit staphylococcal and enterococcal biofilm formation. *Antimicrobial Agents and Chemotherapy* **53**:4357–4367 DOI 10.1128/AAC.00077-09.

Peulen TO, Wilkinson KJ. 2011. Diffusion of nanoparticles in a biofilm. *Environmental Science & Technology* **45**:3367–3373 DOI 10.1021/es103450g.

Punjabi K, Mehta S, Chavan R, Chitalia V, Deogharkar D, Deshpande S. 2018. Efficiency of biosynthesized silver and zinc nanoparticles against multi-drug resistant pathogens. *Frontiers in Microbiology* **9**:2207 DOI 10.3389/fmicb.2018.02207.

Raza MA, Kanwal Z, Rauf A, Sabri AN, Riaz S, Naseem S. 2016. Size- and shape-dependent antibacterial studies of silver nanoparticles synthesized by wet chemical routes. *Nanomaterials* **6**:74 DOI 10.3390/nano6040074.

Sá MCA, Oliveira SAS, Dantas EM, Gouveia GV, Gouveia JJS, Veschi JLA, Costa MM. 2018. Resistance of *Corynebacterium pseudotuberculosis* in the Brazilian semiarid environment. *Pesquisa Veterinaria Brasileira* **38**:1091–1096 DOI 10.1590/1678-5150-PVB-4960.

Sá MCA, Veschi JLA, Santos GB, Amanso ES, Oliveira AS, Veneroni-Gouveia RAMG, Costa MM, Veschi JLA, Santos GB, Amanso ES, Oliveira SAS, Mota RA. 2013. Activity of disinfectants and biofilm production of *Corynebacterium pseudotuberculosis*. *Pesquisa Veterinaria Brasileira* **33**:1319–1324 DOI 10.1590/S0100-736X2013001100006.

Saising J, Dube L, Ziebandt AK, Voravuthikunchai SP, Nega M, Götz F. 2012. Activity of gallidermin on *Staphylococcus aureus* and *Staphylococcus epidermidis* biofilms. *Antimicrobial Agents and Chemotherapy* **56**:5804–5810 DOI 10.1128/AAC.01296-12.

Santos LM, Rodrigues DM, Kalil MA, Azevedo V, Meyer R, Umsza-Guez MA, Machado BA, Seyffert N, Portela RW. 2021. Activity of ethanolic and supercritical propolis extracts in *Corynebacterium pseudotuberculosis* and its associated biofilm. *Frontiers in Veterinary Science* **8**:700030 DOI 10.3389/fvets.2021.700030.

Santos LM, Stanisic D, Menezes UJ, Mendonça MA, Barral TD, Seyffert N, Azevedo V, Durán N, Meyer R, Tasic L, Portela RW. 2019. Biogenic silver nanoparticles as a post-surgical treatment for *Corynebacterium pseudotuberculosis* infection in small ruminants. *Frontiers in Microbiology* **10**:824 DOI 10.3389/fmicb.2019.00824.

Shrestha L, Hai-Ming F, Hui-Ren T, Jian-Dong H. 2022. Recent strategies to combat biofilms using antimicrobial agents and therapeutic approaches. *Pathogens* **11**:292 DOI 10.3390/pathogens11030292.

Siddique MH, Aslam B, Imran M, Ashraf A, Nadeem H, Hayat S, Khurshid M, Afzal M, Malik IR, Shahzad M, Qureshi U, Khan ZUH, Muzammil S. 2020. Effect of silver nanoparticles on biofilm formation and EPS production of multidrug-resistant *Klebsiella pneumoniae*. *Biomedical Research* **2020**:6398165 DOI 10.1155/2020/6398165.

Singh BR, Singh BN, Singh A, Khan W, Naqvi AH, Singh HB. 2015. Mycofabricated biosilver nanoparticles interrupt *Pseudomonas aeruginosa* quorum sensing systems. *Scientific Reports* **5**:13719 DOI 10.1038/srep13719.

Stanisic D, Fregonesi NL, Barros CHN, Pontes JGM, Fulaz S, Menezes UJ, Nicoleti JL, Castro TLP, Seyffert N, Azevedo V, Durán N, Portela RW, Tasic L. 2018. NMR insights on nano silver post-surgical treatment of superficial caseous lymphadenitis in small ruminants. *RSC Advances* **8**:40778–40786 DOI 10.1039/c8ra08218a.

Subhadra B, Kim DH, Woo K, Surendran S, Choi CH. 2018. Control of biofilm formation in healthcare: recent advances exploiting quorum-sensing interference strategies and multidrug efflux pump inhibitors. *Materials* **11**:1676 DOI 10.3390/ma11091676.

Tăbăran AF, Matea CT, Mocan T, Tăbăran A, Mihaiu M, Iancu C, Mocan L. 2020. Silver nanoparticles for the therapy of tuberculosis. *International Journal of Nanomedicine* **15**:2231–2258 DOI 10.2147/IJN.S241183.

Trevisan DAC, Silva AF da, Negri M, Abreu Filho BA de, Machinski Junior M, Patussi EV, Campanerut-Sá PAZ, Mikcha JMG. 2018. Antibacterial and antibiofilm activity of carvacrol against *Salmonella enterica* serotype Typhimurium. *Brazilian Journal of Pharmaceutical Sciences* **54**:e17229 DOI 10.1590/s2175-97902018000117229.

Vestby LK, Grønseth T, Simm R, Nesse LL. 2020. Bacterial biofilm and its role in the pathogenesis of disease. *Antibiotics* **9**:59 DOI 10.3390/antibiotics9020059.

Williamson LH. 2001. Caseous lymphadenitis in small ruminants. *Veterinary Clinics of North America: Food Animal Practice* **17**:359–371 DOI 10.1016/S0749-0720(15)30033-5.

Wong EHJ, Ng CG, Goh KL, Vadivelu J, Ho B, Loke MF. 2018. Metabolomic analysis of low and high biofilm-forming *Helicobacter pylori* strains. *Scientific Reports* **8**:1409 DOI 10.1038/s41598-018-19697-0.

Zhang YQ, Wu QP, Zhang JM, Yang XH. 2011. Effects of ozone on membrane permeability and ultrastructure in *Pseudomonas aeruginosa*. *Journal of Applied Microbiology* **111**:1006–1015 DOI 10.1111/j.1365-2672.2011.05113.x.